PAPER

NJC
www.rsc.org/njc

Rapid synthesis of nanoparticles of hexagonal type In_2O_3 and spherical type Tl_2O_3 by microwave irradiation

Chitta Ranjan Patra and Aharon Gedanken*

Department of Chemistry, Bar-Ilan University, Ramat-Gan 52900, Israel.
E-mail: gedanken@mail.biu.ac.il; Fax: +972-3-535-1250; Tel: 972-3-531-8315

Received (in Montpellier, France) 7th January 2004, Accepted 24th March 2004
First published as an Advance Article on the web 16th July 2004

Semiconducting nanoparticles of indium and thallium oxides (In_2O_3 and Tl_2O_3) have been successfully synthesized in high yield ($>95\%$) by microwave irradiation. The oxides are synthesized in a simple domestic microwave oven (DMO) by adding an aqueous ammonia solution to the aqueous solutions of indium chloride ($InCl_3$) and thallium chloride ($TlCl_3$), respectively. The structures, morphologies, compositions and physical properties of the products have been characterized by powder X-ray diffraction (XRD), thermogravimetric analysis (TGA), differential scanning calorimetry (DSC), energy dispersive X-ray (EDX) analysis, transmission electron microscopy (TEM), selected area electron diffraction (SAED), *etc.* The XRD and SAED analysis indicate that the as-synthesized product, obtained after microwave (MW) heating of the indium chloride solution, is crystalline $In(OH)_3$, but its calcined form is a crystalline body-centered cubic (bcc) phase of In_2O_3. On the other hand, in the case of thallium chloride, the as-synthesized material is a crystalline body-centered cubic (bcc) phase of Tl_2O_3. The particles are of uniform size, being about 16 nm and 24 nm for Tl_2O_3 and In_2O_3, respectively. A possible mechanism for the formation of the In_2O_3 and Tl_2O_3 nanoparticles is discussed briefly.

Introduction

Indium oxide, a transparent conducting oxide (with a direct band gap of about 3.6 eV and an indirect band gap of about 2.6 eV), has been widely used in the electronics field for applications such as anti-static coatings, light detection, gas sensors for ozone and nitrogen dioxide, photoelectrode materials, solid electrolyte cells, solar cells, transparent conductive electrodes in electronic devices for liquid crystal displays (LCD), photovoltaic devices, UV lasers and detectors,[1,2] *etc.* On the other hand, thallium is generally regarded as a toxic metal, but thallium is most well-known for the usage of its sulfate as a rat and ant killer. Various thallium compounds have been used for the treatment of ringworm and other skin infections[3] and as a chemical tracer in diagnosis, particularly in cardiology.[4] Thallium compounds are also used for X-ray, γ-ray and infrared detectors.[5,6] A very narrow window between therapeutic and toxic behavior limits their medical use. Thallium is a very important ingredient of many high-temperature oxide superconductors[7] due to the wide range of stoichiometries over which superconductivity is observed in such thallium-doped materials.[8] Because of such promising applications of In_2O_3 and Tl_2O_3, it is very important to be able to fabricate their nanoparticles in crystalline form using a very simple method.

Recently, these semiconducting nanomaterials have generated tremendous interest in both scientific research and engineering fields. The electronic and optical properties of nanoparticles strongly depend on their size and dimensionality.[9] Nanometer-sized In_2O_3 shows obvious differences in its optical properties (*e.g.*, optical band gap and luminescence properties) relative to bulk In_2O_3.[10,11] Therefore, it is important to synthesize small nanoparticles (In_2O_3, Tl_2O_3) that can meet the demands of further applications. Due its numerous applications, indium oxide particles of nanometer size have been extensively synthesized by several techniques such as (a) thermal evaporation,[12,13] (b) template method,[14] (c) pulsed laser deposition technique,[15] (d) vapor phase transport and condensation deposition process,[16] (e) carbothermal reduction,[17] (f) decomposition of the organometallic precursor,[18] (g) microemulsion method,[19] (h) sonochemical method,[20] *etc.* There are a few reports on the synthesis of nano-sized Tl_2O_3 using thermal decomposition,[21] electrodeposition[22,23] and sonochemical[24] methods. However, the above-mentioned methods for the synthesis of In_2O_3 and Tl_2O_3 face many kinds of problems: (i) methods (a), (d) and (e) need very high temperatures $>1000\,^{\circ}C$ and long heating times; (ii) method (b) needs a template and a long reaction time (>5 h); (iii) method (c) needs special instrumentation and the product deposition is carried out at $250\,^{\circ}C$ under an oxygen pressure of 10 mTorr; (iv) method (f) needs [In(η^5-C_5H_5)], an organometallic source of indium, which itself is an expensive starting material; (v) method (g) needs an anionic surfactant; (vi) with method (h) fullerene-like Tl_2O (but not Tl_2O_3) is obtained from an aqueous solution of $TlCl_3$ under an argon atmosphere. (vii) Two nanoproducts, In_2S_3 and In_2O_3, are obtained when an aqueous solution of $InCl_3$ is reacted with thioacetamide, and their ratio is found to depend on the sonication temperature. These problems are the limiting factors in the development of an efficient synthesis of In_2O_3 and Tl_2O_3 nanoparticles. To avoid these problems, we have developed an efficient and very simple method for the synthesis of In_2O_3 and Tl_2O_3 nanoparticles conducted in a simple domestic microwave oven (DMO). The microwave-assisted products are pure, structurally uniform, highly crystalline and are obtained in high yield; furthermore, this method does not need high temperature, high pressure, any catalyst, template, surfactant, vacuum conditions or preprocessing. Additionally, this method is simple, fast, clean, efficient, cheap, economical, non-toxic, and eco-friendly. It also may be extended to fabricate many other nanoscale materials.

In exploring the solvothermal method as a route for the synthesis of metal oxides (*e.g.*, nano In_2O_3, Tl_2O_3), we have chosen water as a solvent. Reactions are conducted using microwave heating for their activation. In these reactions the

DOI: 10.1039/b400206g

temperature is a dominant factor in affecting the reactivity. The microwave heating technique is specially known as a high temperature activating method. In the case of microwave irradiation there are two main modes of action. The first, which occurs in the liquid phase, is an interaction between the high-frequency electromagnetic radiation (2.45×10^9 Hz) and the permanent dipole moment of the molecule, resulting in molecular rotations, which bring about rapid volumetric heating of the liquid phase. Water is an excellent susceptor of the microwave radiation because of its high permanent dipole (dielectric constant, $\varepsilon = 80.4$), which makes it one of the best solvents for microwave-assisted reactions.[25] In the second mode, metallic particles, produced as intermediates in the water solvent, are also good susceptors of the microwave radiation and cause the rapid heating of these particles. The temperature in the reaction container will therefore be much higher than that of the surrounding liquid.

In the present paper, we report a conceptually different and easier technique for the rapid synthesis of a hexagonal type of In_2O_3 and a spherical type of Tl_2O_3 nanoparticles by a simple microwave (MW) route, which, we believe, has never been reported elsewhere.

Experimental

Materials

Indium(III) chloride (Aldrich, 99.9% purity), thallium(III) chloride (Aldrich, 99.9% purity), ammonium hydroxide (BIO LAB Ltd., AR grade, 24% v/v aqueous solution), were used as received without further purification.

Synthesis

In a typical synthesis, 0.221 g (1 mM) of indium(III) chloride or 0.310 g (1 mM) thallium(III) chloride salts in 40 g of distilled water were placed in a 100 ml round-bottomed flask and then 10 ml of the ammonium hydroxide solution was added. The sample was irradiated simultaneously for 60 min, without further addition of the ammonia solution, with 60% of the instrument's power (*i.e.*, on/off irradiation cycles were in the ratio of 3:2) in open air atmosphere. This cycling mode (60% of cycling mode: 12 s on and 7 s off) was chosen in order to control the reaction and reduce the risk of superheating the solvent. The reaction yielded 0.16 g and 0.22 g of as-synthesized products, which corresponds to 96.3% and 96.5% yields of $In(OH)_3$ and Tl_2O_3, respectively. The microwave refluxing apparatus was a modified domestic microwave oven (900 W, with a working frequency of 2.45 GHz), which has been described elsewhere.[26] A blank experiment was also carried out separately with an aqueous solution of indium(III) chloride or thallium(III) chloride without added ammonia solution under similar microwave reaction conditions. No noticeable precipitation was formed in each case after the solution was irradiated for more than 1 h.

In another control experiment, we heated a 1 mM aqueous solution of $InCl_3$ or $TlCl_3$ to 300 °C in a high-pressure cell, without microwave heating. No observable powder formation occurred after the solution was heated, even for 4 h. Table 1 summarizes the various reaction conditions under microwave irradiation. In the post-reaction treatment, the resulting products were collected, centrifuged at 9000 rpm, washed several times using ethanol and distilled water, and then dried overnight under vacuum at room temperature. A part of the as-synthesized material, obtained from MW heating of the aqueous solution of $InCl_3$, was annealed under air for 4 h at 700 °C to develop the desired phase. The above experiments were conducted several times and showed good reproducibility.

Characterization

The structure and phase purity of the as-synthesized and calcined samples were determined by X-ray diffraction (XRD) analysis using a Bruker AXS D8 Advance Powder X-ray diffractometer (using CuKα $\lambda = 1.5418$ Å radiation) operating at 40 kV and 40 mA, with a graphite reflected-beam monochromator and variable divergence slits. Peak fitting and lattice parameter refinement were computed using the Topas and Metric programs (Bruker Analytical X-ray System). EDX measurements were done on an X-ray microanalyzer (Oxford Scientific) built on a JSM-840 scanning electron microscope (JEOL). The surface area was measured by N_2 adsorption and calculated using the BET equation in a Micrometrics Gemini instrument. To determine the percentage of hydrogen, elemental analysis was carried out on an EA 1110 CHNS–O CE Instruments. Thermogravimetric analysis (TGA) of the as-synthesized sample was carried out under a stream of nitrogen at a heating rate of 5 °C min^{-1} from 25 to 1000 °C using a Mettler TGA/STDA 851. Differential scanning calorimetric (DSC) analysis of the as-synthesized sample was carried out on a Mettler Toledo TC 15 using a stream of nitrogen (20 ml min^{-1}) at a heating rate of 5 °C min^{-1} on the sample in a crimped aluminium crucible from 20 °C up to 600 °C. The particle morphology (microstructure of the samples) was studied with low-resolution transmission electron microscopy (LRTEM), which was done on a JEOL-JEM 100SX microscope, working at a 100 kV accelerating voltage. High-resolution TEM (HRTEM) images were taken using a JEOL 2010 with 200 kV accelerating voltage. Samples for TEM were prepared by placing a small quantity of the sample in ethanol and sonicating for 10 min in a vial in a sonication bath. One or two drops of the sample suspension (nanoparticle solution) were deposited on a copper grid (400 mesh, Spi Suppliers, West Chester, PA, USA) coated with carbon film. Whatmann filter paper on the grid absorbed the droplet and dried the excess solvent in 5–10 min.

Table 1 Experimental conditions[a] for the preparation of indium(III) oxide and thallium(III) oxide nanoparticles under microwave irradiation

			pH			
Entry	Metal salt	Aqueous ammonia soln/ml	Initial	Final	XRD product	Morphology from TEM
1	$InCl_3$	–	–	–	–	–
2	$TlCl_3$	–	–	–	–	–
3	$InCl_3$	10	9.0	4.5	Crystalline	Nanosheets
4	$TlCl_3$	10	9.0	4.5	Crystalline	Spherical nanoparticles
5	Crystalline indium hydroxide (entry 3) annealed at 700 °C in air for 4 h				Crystalline	Hexagonal nanoparticles

[a] Reaction conditions: microwave heating in an open air atmosphere using 1 mM of indium(III) chloride or 1 mM of thallium (III) chloride, 40 g of distilled water, with or without 10 ml of aqueous NH_4OH soln. Irradiation time = 60 min.

Results and discussion

X-Ray diffraction studies

Fig. 1 shows the XRD patterns of the as-synthesized and calcined products of the MW irradiation of an aqueous solution of $InCl_3$. Trace a depicts the XRD patterns of as-synthesized crystalline $In(OH)_3$ material (entry 3 in Table 1; it matches with JCPDS, Powder Diffraction File No. 76-1463), whereas trace b represents the XRD patterns of its calcined form (In_2O_3) heated at 700 °C in air for 4 h. All the reflections in this trace can be indexed to the body-centered cubic (bcc) phase of In_2O_3 with lattice parameters $a = b = c = 10.1$ Å, in good agreement with the reported values of In_2O_3 in the literature (JCPDS, Powder Diffraction File No. 71-2194). Trace c in Fig. 1 illustrates the diffraction pattern of the as-synthesized sample obtained from microwave heating of an aqueous $TlCl_3$ solution (entry 4 in Table 1). The diffraction peaks in this trace can be indexed to a body-centered cubic (bcc) phase of Tl_2O_3 with lattice parameters $a = b = c = 10.5$ Å, which is consistent with the standard value for the bulk cubic phase of Tl_2O_3 (JCPDS Card. No. 33-1404). In both traces b and c no peaks associated with other crystalline forms of In_2O_3 or Tl_2O_3 are detected. This result suggests that as-synthesized Tl_2O_3 and calcined In_2O_3 contain only one crystalline phase and other crystalline phases either do not exist or are below the detection level. The broad peaks indicate that the products are nanosized. The particle sizes of nanocrystals are calculated with the Debye–Scherrer (DS) equation[27] and are found to be in the range of 22–24 nm for the calcined In_2O_3 sample and 14–17 nm for the as-synthesized Tl_2O_3 sample. The calculated particle sizes by XRD for both the samples are given in Table 2.

Thermogravimetric (TG) and differential scanning calorimetric (DSC) measurements

In order to characterize the nature of the as-synthesized $In(OH)_3$ product (entry 3 in Table 1 and entry 1 in Table 2) obtained by the MW heating of an aqueous $InCl_3$ solution, both TGA and DSC measurements are carried out. Fig. 2 shows the weight loss of the as-synthesized particles as a function of temperature. TGA shows two distinct weight loss steps, with an overall weight loss of 21% between 30 °C and 500 °C. The lower weight loss (5 wt %) is observed between 30 °C and 150 °C, which can occur from the evaporation of physically adsorbed water and ammonia from the surface of the as-synthesized material. The greater weight loss (16 wt %) by TGA that is observed between 150 °C to 500 °C may be due to the decomposition of $In(OH)_3$ to In_2O_3 [the theoretical weight loss for the conversion of $In(OH)_3$ to In_2O_3 is 16.3 wt %], which corroborates the reported literature.[28] The process can be represented as:

$$2In(OH)_3(s) = In_2O_3(s) + 3H_2O(g) \uparrow \qquad (a)$$

This result indirectly proves that the as-synthesized product obtained from the MW heating of an aqueous $InCl_3$ solution is $In(OH)_3$.

The differential scanning calorimetric (DSC) pattern of the as-synthesized product is shown in Fig. 3. The endothermic spectrum from 30 °C to 100 °C indicates the desorption of water molecules from the surface of the nanoparticles. The endotherm around 100 °C to 260 °C is attributed to the transformation of $In(OH)_3$ to In_2O_3 according to eqn. (a), which is a endothermic reaction. The enthalpy for this reaction is $\Delta H_{298\ K} = 74.17 \pm 2.7$ kJ mol^{-1}.[29] The exotherm around 260 °C to 400 °C is due to the crystallization of In_2O_3. The exothermic peak disappears when the sample is reheated in the same temperature range. The end product of the TGA and DSC measurements is In_2O_3, as inferred from the XRD results.

To prove the existence of hydrogen in the as-synthesized sample (entry 1 in Table 2), a CHN analysis was performed. The elemental analysis of the as-synthesized sample gives 1.9 wt % of hydrogen, compared with the theoretical value of 1.8 wt % in $In(OH)_3$. Thus, XRD, elemental analysis, and TGA and DSC experiments all prove that the as-synthesized material is $In(OH)_3$ and its calcined form is In_2O_3.

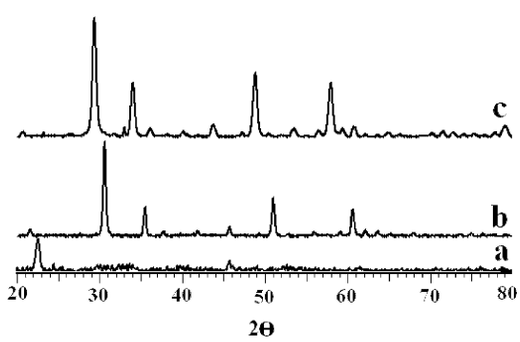

Fig. 1 X-Ray diffraction pattern of (a) as-synthesized $In(OH)_3$ nanoparticles, (b) calcined In_2O_3 nanoparticles and (c) as-synthesized Tl_2O_3, synthesized by microwave heating.

BET measurements

The surface area of the as-synthesized materials and calcined material were measured by N_2 adsorption and calculated using the BET equation; they were found to be 25, 21 and 75 m^2 g^{-1} for the as-synthesized $In(OH)_3$, Tl_2O_3, and calcined In_2O_3, respectively. The lower value of the surface area of $In(OH)_3$ may be due to the aggregated nature of the crystalline product that disintegrates upon annealing. The high surface area of In_2O_3 is due to uniformly monodispersed crystalline nanoparticles. The chemical composition of the samples is analyzed by energy dispersive X-ray (EDX) analysis. The physicochemical characteristics of the as-synthesized and annealed samples are given in Table 2.

Transmission electron microscopy (TEM)

The low-resolution transmission electron microscopy (LRTEM) and high-resolution transmission electron microscopy (HRTEM) observations for the as-synthesized and calcined nanoparticles are shown in Figs. 4 and 5. Fig. 4(A) indicates that the as-synthesized $In(OH)_3$ material is crystalline

Table 2 Particle size, BET surface area, EDX and H analysis of microwave-assisted synthesized indium(III) oxide and thallium(III) oxide materials

Entry	Product	Particle size/nm from XRD	Particle size/nm from TEM	EDX stoichiometry	H analysis/wt %	BET surface area/m^2 g^{-1}
1	$In(OH)_3$[a]	–	–	$In(OH)_3$	1.9	25.0
2	In_2O_3[b]	22–24	22–23	In_2O_3	–	74.9
3	Tl_2O_3[c]	14–17	15–16	Tl_2O_3	–	21.0

[a] As-synthesized $In(OH)_3$ material collected after 60 min of microwave reaction time. [b] Calcined form of In_2O_3: 700 °C for 4 h in the presence of air. [c] As-synthesized crystalline Tl_2O_3 material collected after 60 min of microwave reaction time.

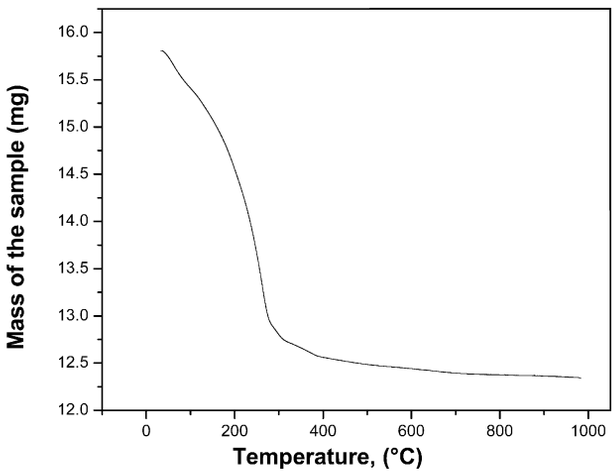

Fig. 2 Thermogravimetric analysis of the as-synthesized $In(OH)_3$, synthesized by microwave heating.

in nature (confirmed by XRD) and has a nanosheet-like structure. These uniform nanosheets are converted into In_2O_3 nanoparticles upon calcination, as shown in the HRTEM images of Fig. 4(B)–4(E). It is observed that the In_2O_3 particles are crystalline with a particle size of *ca.* 22–23 nm. The particles are hexagonal in shape with a uniform size. The size matches the value calculated by the Debye–Scherrer equation from the XRD data. The nanosize of the In_2O_3 particles is evidenced from both the BET and TEM measurements. In addition we have conducted DRS (diffused reflection spectroscopy) studies of the In_2O_3 nanoparticles. An absorption peak is detected at 305 nm. The reflection (absorption) peak is blue-shifted by 20 nm as compared with ref. 10 (particle size of 80 nm). This is a further indication of the small size of our particles.

In order to obtain the detailed structure and composition of the calcined In_2O_3 material (entry 2 in Table 2), EDX, HRTEM and SAED measurements were carried out. Fig. 4(D) and 4(E) show the HRTEM lattice images of a few In_2O_3 nanoparticles with a magnification of 390 000 and 650 000, respectively. It is seen that the lattice fringes of the (211) planes are spaced by 0.415 nm, compared with the theoretical interplanar spacing of 0.413 nm for the body-centered cubic In_2O_3phase. Fig. 4(D)–4(F) also reveal that these nanoparticles are single crystalline and that the examined region is free of dislocation and staking faults. The corresponding SAED pattern is shown in Fig. 4(F), which shows that the

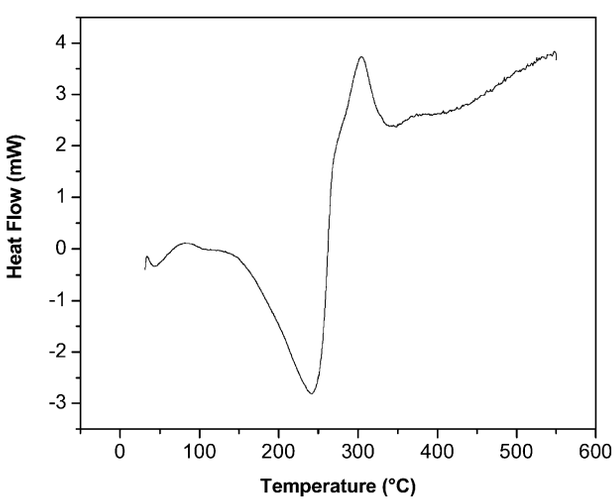

Fig. 3 Differential scanning calorimetry (DSC) analysis of the as-synthesized $In(OH)_3$, synthesized by microwave heating.

calcined material is crystalline and can be indexed to body-centered, cubic phase In_2O_3 nanoparticles. The EDX measurement of an individual particle indicates that the particle is composed of 82.6 wt % of indium and 17.4 wt % of oxygen, compared to the theoretical values of In = 82.7 wt % and O = 17.3 wt %. Thus, the XRD pattern (JCPDS Card. No. 06-0180), EDX analysis and the SAED pattern all indicate that the calcined material is stoichiometric In_2O_3.

Fig. 5(A) shows an HRTEM image revealing the general morphology of as-synthesized crystalline Tl_2O_3. It can be seen that the sample consists of mainly spherical nanoparticles of a diameter of 15–16 nm, which matches the value calculated by the Debye–Scherrer equation from the XRD data. It is observed that the nanoparticles with uniform size are held together. The detailed structure and composition of individual as-synthesized Tl_2O_3 nanoparticles have been characterized using HRTEM and SAED. A representative HRTEM image [Fig. 5(B)] of a single spherical particle of as-synthesized Tl_2O_3 shows the lattice planes with a clearly resolved interplanar distance of $d_{222} = 0.31$ nm, compared with a theoretical interplanar spacing of 0.3042 nm. The intense rings detected in the corresponding SAED pattern [Fig. 5(C)] are indexed to body-centered cubic Tl_2O_3. Thus, XRD (JCPDS Card. No. 33-1404) and SAED patterns together indicate that the as-synthesized material is stoichiometric Tl_2O_3.

Mechanism

$In(OH)_3$ and Tl_2O_3 have been synthesized by refluxing a mixture of an aqueous solution of $InCl_3$ or $TlCl_3$ with an aqueous NH_4OH solution under microwave irradiation. Control experiments with an aqueous solution of $InCl_3$ or $TlCl_3$ without an ammonia solution under similar microwave reaction conditions did not yield any noticeable precipitation after the solutions were irradiated for more than 1 h. These results indicate that the reaction occurs only under basic conditions. Thus, ammonia is the key factor for the formation of $In(OH)_3$ and Tl_2O_3.

Our proposed mechanism for the formation of indium hydroxide and thallium oxide can be represented by the following equations:

$$M_{(aq)}{}^{3+} + 3H_2O_{(l)} \leftrightarrow M(OH)_{3(s)} + 6H_{(aq)}{}^{+} \quad [M = In,\ Tl] \tag{1}$$

$$2M(OH)_3(s) \rightarrow M_2O_3\ (s) + 3H_2O(g) \uparrow \tag{2}$$

The hydrolysis of indium chloride or nitrate has been studied at 75 or 120 °C by Yura *et al.*[28] If we consider that the aqueous ions (In^{3+} or Tl^{3+}) will undergo hydrolysis by the following equation:

$$[M^{III}(H_2O)_6]^{3+} \leftrightarrow [M^{III}(H_2O)_5(OH)]^{2+} + H^{+}(aq) \tag{3}$$

the hydrolysis constants (k_h) for indium and thallium are 2×10^{-4} and $\sim 7 \times 10^{-2}$, respectively.[30] Although the hydrolysis of indium and thallium chloride occurs at relatively low temperatures, it does not yield $In(OH)_3$ and Tl_2O_3 (without microwave heating) at temperatures lower than 75 °C. However, according to our control experiments, $In(OH)_3$ or Tl_2O_3, the non-soluble products, are not formed even at 300 °C. The formation of $In(OH)_3$ and Tl_2O_3 from $InCl_3$ and $TlCl_3$, respectively, results from the high temperatures developed locally during microwave irradiation. Our interpretation is that these endothermic reactions are driven by the high local temperatures created by the microwave heating, which may be the driving force for the formation of In and Tl oxides in aqueous media. Following Le Chatelier's principle, the importance of base is also made clear in eqn. (1). The pH change from

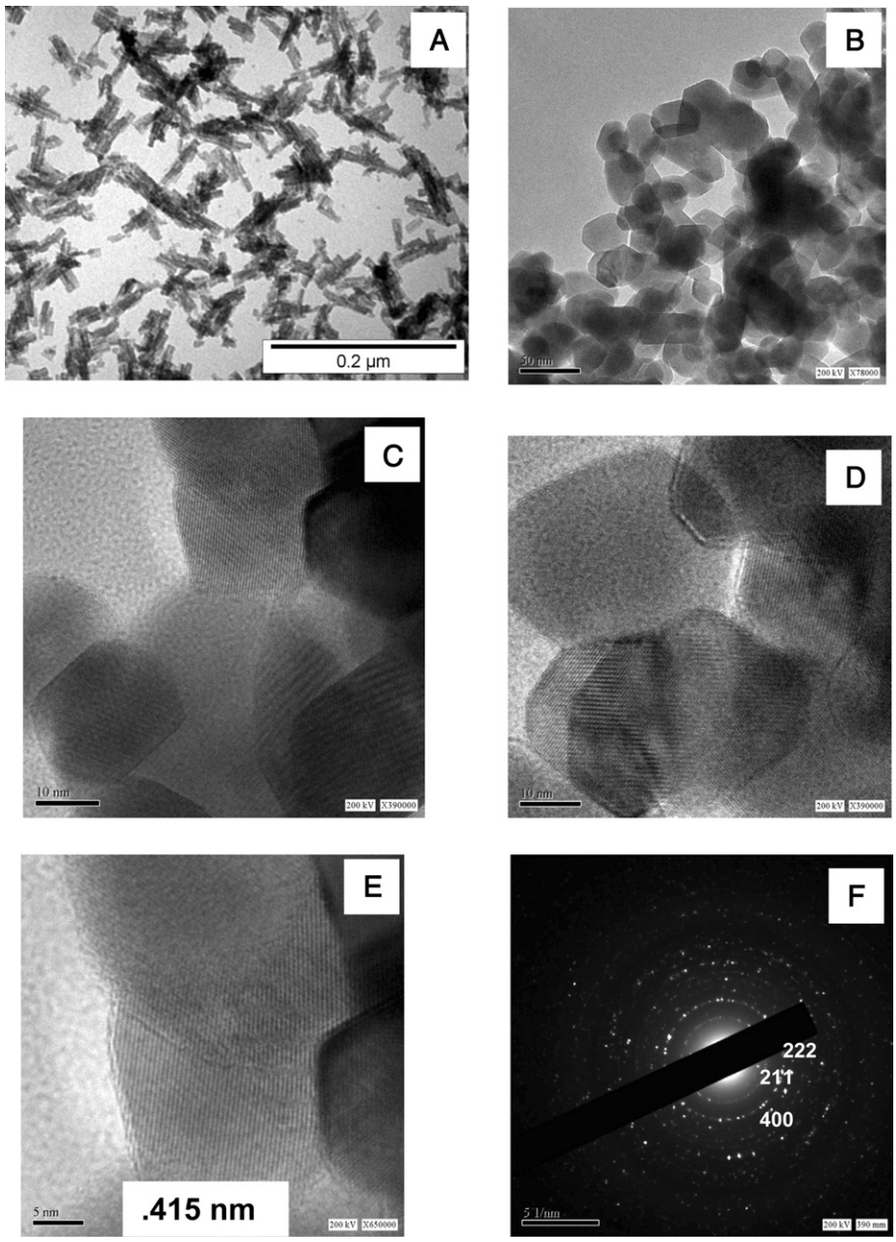

Fig. 4 Low-resolution transmission electron microscopy (LRTEM) image of (A) as-synthesized $In(OH)_3$ nanoparticles with a magnification of 250 000. (B, C, D) High-resolution transmission electron microscopy (HRTEM) images of calcined In_2O_3 nanoparticles. (E) HRTEM lattice image of an individual hexagonal In_2O_3 nanoparticle with a magnification of 650 000 in which the lattice planes (211) are clearly resolved. (F) corresponding selected area electron diffraction pattern of an individual In_2O_3 nanoparticle.

pH = 9.0 to 4.5 after microwave heating (see Table 1) also supports our hypothesis.

Finally, it is observed that after the direct microwave treatment, indium hydroxide [$In(OH)_3$] and thallium oxide (Tl_2O_3) are formed in the case of the indium and thallium systems, respectively. We can try to explain the probable reason in the following way. In the presence of ammonia, aqueous solution of $M^{III}Cl_3$ (M = In and Tl) gives initially $M^{III}(OH)_3$, but on heating $M^{III}(OH)_3$ can covert into M_2O_3. Now, In_2O_3 is an amphoteric oxide (dissolves in both acids and bases) but Tl_2O_3 is a basic oxide, according to Fajans' polarizing ability. In the presence of ammonia, In_2O_3 forms $In(OH)_3$ (stable in alkaline solution due to the amphoteric nature of In_2O_3), because of the larger size and lesser electronegativity of indium compared to gallium. On the other hand, the addition of ammonia to an aqueous solution containing thallic salts gives stable Tl_2O_3 from dehydration of $Tl(OH)_3$. For the higher members of the 18 shell subgroups (Ga, In and Tl belong to the 18 shell elements in the periodic table) to resist the use of the s electrons in polar bond formation, thallium possesses what Sidgwick called the "inert pair." There appears to be no definite $Tl(OH)_3$.[31,32]

Conclusions

$In(OH)_3$ and Tl_2O_3 nanoparticles have been successfully synthesized on a large scale by refluxing a mixture of an aqueous solution of $InCl_3$ or $TlCl_3$ with an NH_4OH solution by microwave heating in a simple domestic microwave oven. In the absence of microwave irradiation, these nanoparticles are not formed. On heating, $In(OH)_3$ is converted into In_2O_3. Microwave heating provides an effective and rapid method for the synthesis of nanocrystalline In_2O_3 and Tl_2O_3 powders because of its homogeneous and fast-heating characteristics. The TEM images show that these particles have uniform sizes of 15–16 nm and 22–23 nm for as-synthesized Tl_2O_3 and calcined In_2O_3, respectively. The XRD, HRTEM and SAED

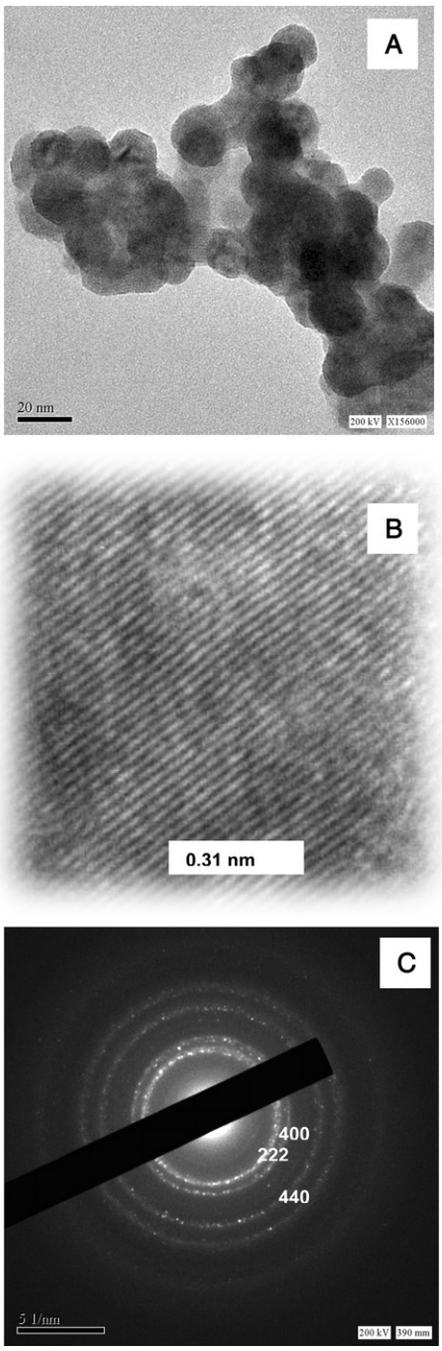

Fig. 5 High-resolution transmission electron microscopy (HRTEM) images of (A) as-synthesized Tl_2O_3 nanoparticles with a magnification of 156 000 and (B) lattice image of an individual spherical Tl_2O_3 nanoparticle with a magnification of 520 000 in which the lattice planes (222) are clearly resolved. (C) corresponding selected area electron diffraction pattern of an individual Tl_2O_3 nanoparticle.

confirm that these nanoparticles are crystalline with a body-centered cubic phase for as-synthesized Tl_2O_3 and calcined In_2O_3 samples. This simple microwave method may be extended to fabricate many other nanoscale materials, such as Ga_2O_3, SnO_2 and ZnO. The synthesized semiconducting oxide nanostructures with different morphologies may have potential applications in optoelectronic nanodevices and nanoscale gas sensors.

Acknowledgements

Dr. C. R. Patra and Prof. A. Gedanken thank the EC for a research grant IST-2001-39112 awarded through the 5th Program of the NANOPHOS Consortium.

References

1 C. G. Granqvist, *Appl. Phys. A: Solid Surf.*, 1993, **57**, 19.
2 I. Hamburg and C. G. Granqvist, *J. Appl. Phys.*, 1986, **60**, R123.
3 D. Moore, I. House and A. Dixon, *Br. Med. J.*, 1993, **306**, 1527.
4 M. D. Cerqueira, C. Maynard, J. L. Ritchie, K. B. Davis and J. W. Kennedy, *J. Am. Coll. Cardiol.*, 1992, **20**, 1452.
5 D. R. Ouimette, R. M. Iodice, P. J. Kung and L. Lynds, *Proc. SPIE-Int. Soc. Opt. Eng.*, 1999, **3770**, 156.
6 J. J. Lee and M. Razeghi, *J. Cryst. Growth*, 2000, **221**, 444.
7 E. P. Khlybov, I. E. Kostyleva, V. I. Nizhankovskii, T. Palewski, J. Warchulska and K. Nenkov, *Physica B (Amsterdam)*, 2001, **294**, 367.
8 R. Sugise and H. Ihara, *Jpn. J. Appl. Phys.*, 1989, **28**, 334.
9 J. Hu, T. W. Odom and C. M. Lieber, *Acc. Chem. Res.*, 1999, **32**, 435.
10 D-B. Yu, S-H. Yu, S-Y. Zhang, J. Zuo, D-B. Wang and Y-T. Qian, *Adv. Funct. Mater.*, 2003, **13**, 497.
11 X. Wu, G. Tang, G. Zhang, B. Zou, B. Yu and W. Chen, *Chin. Sci. Bull.*, 1996, **41**, 635.
12 X. S. Peng, Y. W. Wang, J. Zhang, X. F. Wang, L. X. Zhao, G. W. Meng and L. D. Zhang, *Appl. Phys. A: Mater. Sci. Process.*, 2002, **74**, 437.
13 X. Y. Kong and Z. L. Wang, *Solid State Commun.*, 2003, **128**, 1.
14 H. Cao, X. Qiu, Y. Liang and Q. Zhu, *Appl.Phys. Lett.*, 2003, **83**, 761.
15 S. B. Qadri, H. Kim, M. Yousuf and H. R. Khan, *Appl. Surf. Sci.*, 2003, **208–209**, 611.
16 J. G. Wen, J. Y. Lao, D. Z. Wang, T. M. Kyaw, Y. L. Foo and Z. F. Ren, *Chem. Phys. Lett.*, 2003, **372**, 717.
17 X. C. Wu, J. M. Hong, Z. J. Han and Y. R. Tao, *Chem. Phys. Lett.*, 2003, **373**, 28.
18 K. Soulantica, L. Erades, M. Sauvan, F. Senocq, A. Maisonnat and B. Chaudret, *Adv. Funct. Mater.*, 2003, **13**, 553.
19 X. C. Wu, R. Y. Wang, B. S. Zou, P. F. Wu, J. R. Xu and H. Wei, *J. Vac. Sci. Technol., B*, 1997, **15**, 1889.
20 S. Avivi (Levi), O. Palchik, V. Palchik, M. A. Slifkin, A. M. Weiss and A. Gedanken, *Chem. Mater.*, 2001, **13**, 2195.
21 D. M. Lyons and M. A. Morris, *Cryst. Growth Des.*, 2002, **2**, 427.
22 R. N. Bhattacharya, Z. Xing, J. Z. Wu, J. Chen, S. X. Yang, Z. F. Ren and R. D. Blaugher, *Physica C (Amsterdam)*, 2002, **377**, 327.
23 J. F. Liu, S. X. Wang and K. Z. Yang, *Thin Solid Films*, 1997, **298**, 156.
24 S. Avivi, Y. Mastai and A. Gedanken, *J. Am. Chem. Soc.*, 2002, **122**, 4331.
25 P. Lidström, J. Tierney, B. Wathey and J. Westman, *Tetrahedron*, 2001, **57**, 9225.
26 O. Palchik, I. Felner, G. Kataby and A. Gedanken, *J. Mater. Res.*, 2000, **15**, 2176.
27 *X-Ray Diffraction Procedures*, eds. H. Klug and L. Alexander, Wiley, New York, 1962, p. 125.
28 K. Yura, K. C. Fredrikson and E. Matijevic, *Colloids Surf.*, 1990, **50**, 281.
29 E. H. P. Cordfunke, R. J. M. Konings and W. Ouweltjes, *J. Chem. Thermodyn.*, 1995, **27**, 431.
30 F. A. Cotton and G. Wilkinson, *Advanced Inorganic Chemistry*, John Wiley & Sons, New York, London, 2nd edn., 1966, p. 437.
31 R. T. Sanderson, *Inorganic Chemistry*, Reinhold Publishing Corporation, New York, 1967, ch. 12, p. 179.
32 J. J. Langowski, *Modern Inorganic Chemistry*, Marcel Dekker, Inc., New York, 1973, pp. 290–292.